VNU Journal of Science: Mathematics - Physics

Journal homepage: https://js.vnu.edu.vn/MaP

Original Article

Synthesis of MnO_2/Graphene Nanocomposites using Plasma Electrolysis Method for Photocatalytic Degradation of Methyl Orange Dye in Water

Nguyen Long Tuyen[1,2], Pham Quoc Trieu[1], Nguyen Ngoc Dinh[1], Nguyen Thanh Trung[3], Dang Van Thanh[4,*]

[1]*VNU University of Science, 334 Nguyen Trai, Thanh Xuan, Hanoi, Vietnam*

[2]*Hung Vuong University, Nong Trang, Viet Tri, Phu Tho, Vietnam*

[3]*Institute of Physics, Vietnam Academy of Science and Technology, 18 Hoang Quoc Viet, Cau Giay, Hanoi, Vietnam*

[4]*TNU University of Medicine and Pharmacy, 284 Luong Ngoc Quyen, Thai Nguyen, Vietnam*

Received 9 September 2021
Revised 7 October 2021; Accepted 17 October 2021

Abstract: This report presented an effective way to synthesize MnO_2/graphene nanocomposites using the plasma electrolysis method for photocatalytic degradation of methyl orange dye in water. The morphology, structure, and chemical composition of MnO_2/graphene nanocomposites materials were investigated through scanning electron microscopy (SEM), Raman spectra, and Fourier-transform infrared (FTIR) spectroscopy, respectively. SEM results showed that MnO_2 nanoparticles with particle sizes of 30-50 nm were attached uniformly on the surface of graphene nanosheets. The photodegradation activity was performed under UV-visible irradiation to evaluate the potential application of MnO_2/graphene nanocomposites.

Keywords: Plasma, electrolysis, orange dyes, graphene, MnO_2.

1. Introduction

Methyl orange dye (MOD) is widely used as the colorant and disinfector in rubbers, varnishes, pesticides, dyestuffs, etc. [1, 2]. Subsequently, they are found in colored wastewater from the industries.

* Corresponding author.
E-mail address: thanhdv@tnmc.edu.vn

https//doi.org/10.25073/2588-1124/vnumap.4679

Therefore, the removal of pollutants especially organic dye before discharging mainstream water is necessary. To protect environment, a variety of methods have been conducted, such as ion exchange, adsorption, biological treatment, and photocatalytic degradation [3-5]. Among these approaches, the photocatalytic degradation has drawn much attention due to its effective, low-cost, flexible and less toxic by-product [6-8]. MnO_2 is a kind of transition metal oxide owning to unique properties like eco-friendly material, abundant, low-cost and proper optical behavior. MnO_2 is also known as a semiconducting material with a bandgap energy of 2.3 eV, which can effortlessly be excited under visible light. However, the performance of MnO_2 is still challenging because of its agglomeration and low specific surface area that led to poor photocatalytic performance. To overcome this issue, researchers have combined MnO_2 with two-dimensional materials, especially 2D graphene nanosheets. Several methods have been employed in preparing graphene-MnO_2 nanocomposites, such as soft chemical route, microwave-assisted wet chemical approach, hydrothermal synthesis that requires toxic, high temperature or long processing time [9]. Thus, finding a facile and efficient way for synthesizing MnO_2/graphene nanocomposites is necessary.

Previously, we reported on ultrasonic-assisted plasma electrochemical discharge in the synthesis of graphene nanosheet [10]. This technique is believed to be simple, facile and inexpensive compared to other methods. Adopted with some modifications, one can synthesize MnO_2/graphene nanocomposites. Therefore, in this work, we present a simple one-step route to synthesize MnO_2/graphene nanocomposites by plasma electrolysis process and its application in photodegradation of the methyl orange dye in water.

2. Materials and Methods

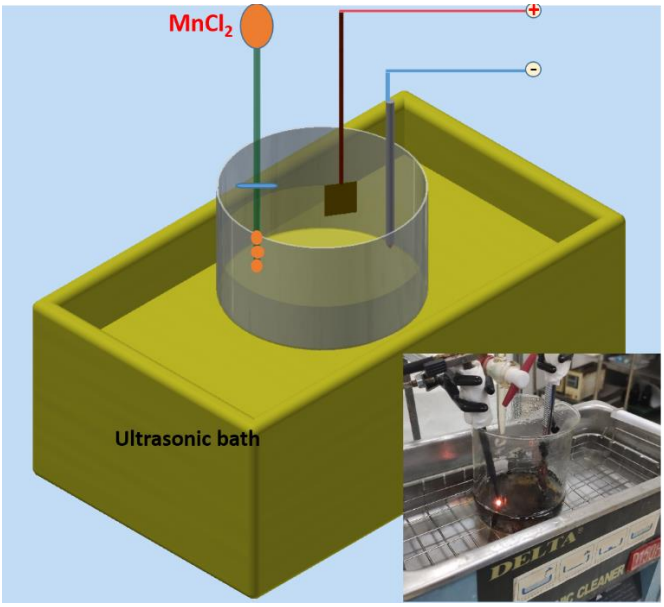

Figure1. Scheme for the synthesis of GMO; inset is the working system image.

MnO_2/graphene nanocomposites were synthesized by ultrasonic-assisted plasma electrochemical discharge method that was reported elsewhere [10]. In detail, the electrolyte was prepared from 200 mL KOH 0.5M under vigorous stirring to gain a homogeneous solution. The 100 mL $MnCl_2$ 0.5M was

prepared and dropwise added with a rate of 2 mL min^{-1}. The DC bias was used to generate an electric field between two electrodes in which tip-formed graphite rod and Pt plate rod are the cathode and anode, respectively. Additionally, the beaker was placed in the ultrasonic bath with a frequency of 40 kHz and a power of 150 W. After 60 minutes, as-prepared samples were achieved by vacuum-assisted filtration through a polyvinylidene fluoride (PVDF) membrane with a pore size of 0.2 μm after being washed with a copious amount of DI water and ethanol. The sample (named as GMO) was further dried at 80 ^oC for 24 h and placed in a desiccator before use. Similarly, the MnO_2 nanoparticles and graphene nanosheets were also conducted in the same process except for using Pt foil as cathode and KOH as an electrolyte, respectively. The schematic diagram of the synthesis of GMO is shown in Figure 1.

The surface morphology was observed by field-emission scanning electron microscopy (FESEM, Hitachi SU8000). Raman spectra were obtained using LabRam HR Evolution spectrometer. Fourier-transform infrared (FTIR) spectra were recorded on a Jasco FT/IR-6700 spectrometer. Methyl orange dye photodegradation was performed under UV-visible irradiation using a 400 W Xenon lamp where the concentration of MOD was 15 ppm. The samples were maintained in the dark for 60 min to complete adsorption at equilibrium, then the suspension was irradiated. After centrifugation, the supernatant was analyzed using an Jasco V-670 absorption spectrometer at λ = 486 nm and the MOD concentrations were estimated using a standard calibration curve.

3. Results and Discussion

The morphologies of MnO_2 nanoparticles and MnO_2/graphene nanocomposites were observed by FE-SEM, the FE-SEM images are shown in Figure 2. The MnO_2 sample shows nanoparticles-like morphology with slight agglomeration (Figure 2a). The agglomeration of MnO_2 can be suppressed on graphene surface as seen in Figure 2b. The size of MnO_2 nanoparticles on graphene surface was found to be in a range of 30-50 nm.

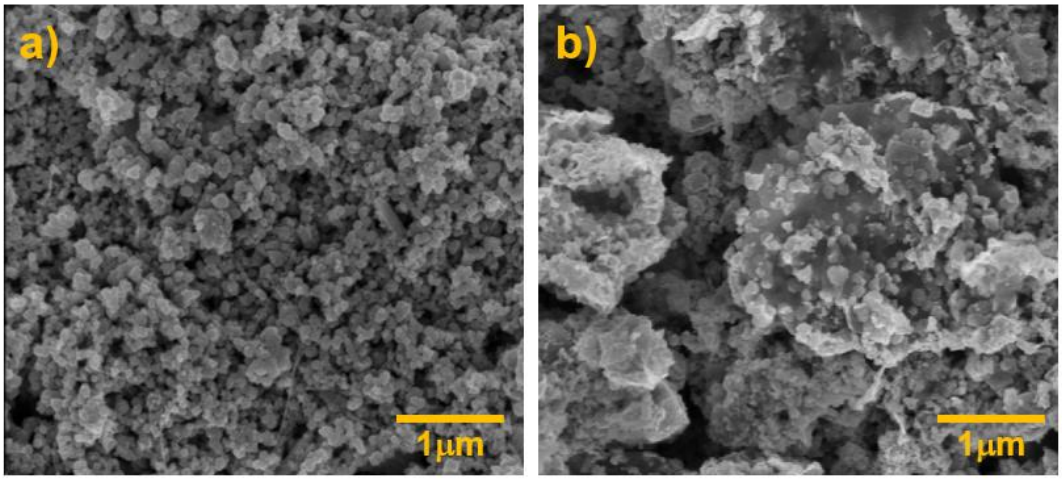

Figure 2. FE-SEM image of (a) MnO_2 and (b) GMO.

As shown in Figure 3, MnO_2/graphene nanocomposites exhibit two main regions. The typical peaks of the graphene material are displayed at 1334, 1584, and 2680 cm^{-1}, which are assigned to the D, G and 2D band, respectively. The dominant peaks are centered at 361 and 648 cm^{-1} corresponding to the Mn-

O symmetric stretching vibration and Mn-O stretching vibration in the MnO_6 group and basal plane of MnO_6, respectively. This is similar to those reported in [11]. Here, the Raman spectra of MnO_2 nanoparticles reveal only their characteristic peaks. As compared with pristine graphene, the peak intensity ratio decreased with the presence of MnO_2 nanoparticles, suggesting graphene nanosheet being depleted. It is remarked that the intensity ratio of D to G band (I_D/I_G) is, in turn, calculated to be of 0.25 and 0.81 for the graphene nanosheet and the MnO_2/graphene nanocomposites. The higher I_D/I_G might be attributed to cracks/defects on the graphene surface and the possibility of formation bonding between MnO_2 and graphene through oxygen bridge.

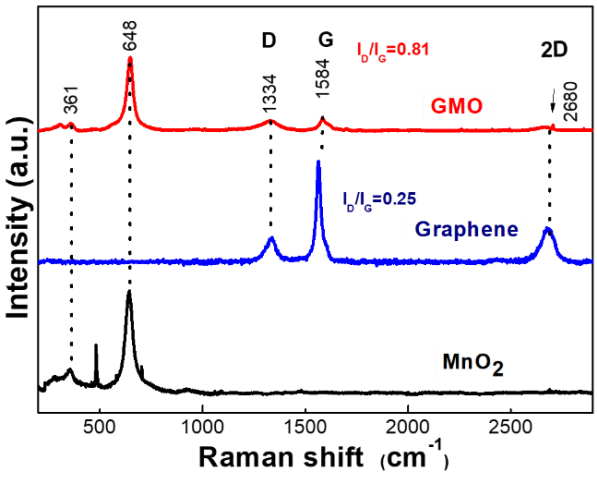

Figure 3. Raman spectra of graphene, MnO_2 and GMO.

FTIR analysis of MnO_2 nanoparticles, graphene nanosheets and MnO_2/graphene nanocomposites are displayed in Figure 4. In the spectrum of graphene nanosheets, the absorption peak at 1580 cm^{-1} corresponds to the stretching vibrations of the aromatic C = C and the absorbed water molecules [12]. In contrast to graphene nanosheets, the new and sharp peaks at 417 and 528 cm^{-1} have occurred in MnO_2/graphene nanocomposite, which can be assigned to the Mn-O bonds of MnO_2 [13]. The spectra of MnO_2 nanoparticles almost show the adsorption peak that is overlapped with whose MnO_2/graphene nanocomposite appeared. Additionally, the peak at 634 cm^{-1} is related to O-Mn-O stretching vibrations [14]. A board adsorption peak at 3398 cm^{-1} indexes to the O-H stretching vibration [15], indicating that the MnO_2 was attached to the graphene surface through chemical bonding. Based on the above characterizations, the one-pot synthesis of MnO_2/graphene was successfully prepared via the plasma electrolysis technique.

The potentially photocatalytic performance of the as-obtained materials was demonstrated by degrading MOD under a Xenon lamp. At a certain reaction interval, the UV–vis spectra of the dye in the solution was measured after irradiating by MnO_2/graphene nanocomposite. The results are shown in Fig. 5. It can be seen that the absorbance intensity is gradually decreased as increasing time in 150 min (Fig. 5a). This implies that the decoloration of methyl orange dye is effective after 120 min. For comparison, the MOD decolorization using MnO_2 is also investigated under a Xenon lamp. The better performance of the MnO_2/graphene nanocomposite is believed to the well-dispersed MnO_2 nanoparticles on graphene surface, the prevention of MnO_2 agglomeration/cluster and enhanced electrical conductivity as well as surface area (Fig. 5b).

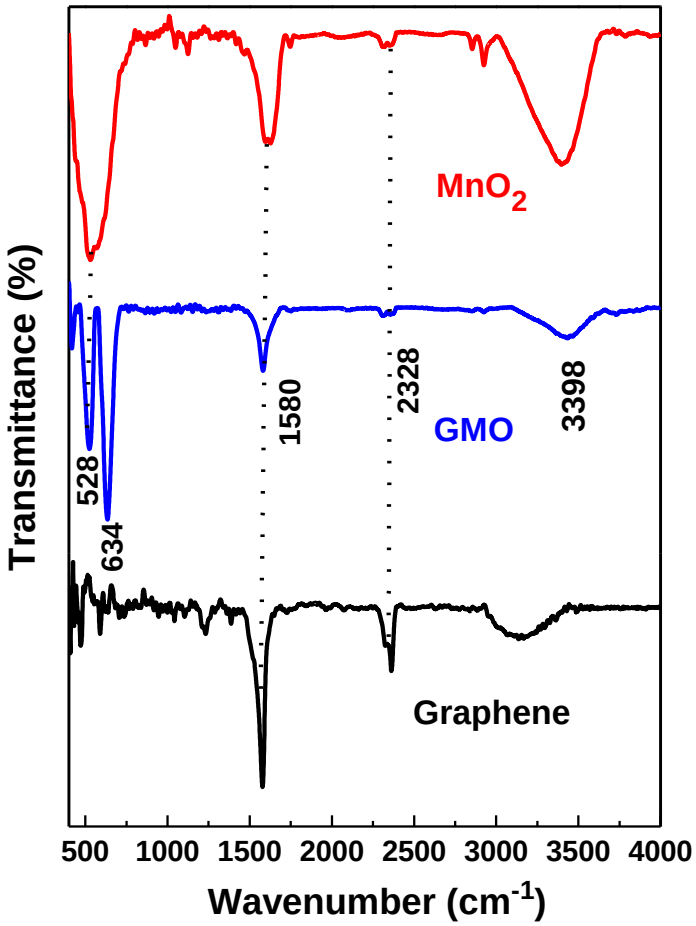

Figure 4. FTIR spectra of graphene, MnO_2 and GMO.

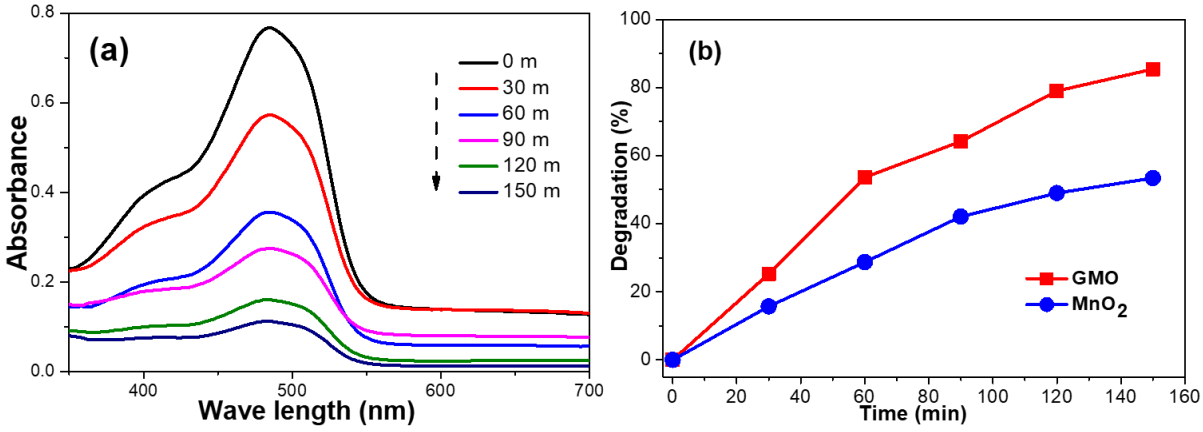

Figure 5. (a) The adsorption spectrum of the orange dye with 10 mg GMO catalyst, pH = 5, (b) photodegradation of MOD by MnO_2 and GMO nanocomposites under Xenon lamp irradiation.

4. Conclusions

A simple one-step route to synthesize MnO_2/graphene nanocomposites by the plasma electrolysis process was successfully developed. The formation of the MnO_2/graphene nanocomposites was confirmed by FT-IR, SEM, and Raman analysis. The degrading methyl orange dye study was performed with a Xenon lamp. It was found that MnO_2/graphene nanocomposites could effectively remove methyl orange dye from water.

Acknowledgments

This research is funded by Vietnam National Foundation for Science and Technology Development (NAFOSTED) under grant number 103.02-2018.40.

References

[1] W. Zhong, T. Jiang, Y. Dang, J. He, S. Y. Chen, C. H. Kuo, D. Kriz, Y. Meng, A. G. Meguerdichian, S. L. Suib, Mechanism Studies on Methyl Orange Dye Degradation by Perovskite-Type $LaNiO_3$-δ under Dark Ambient Conditions, Applied Catalysis A: General, Vol. 549, 2018, pp. 302-309, https://doi.org/10.1016/j.apcata.2017.10.013.

[2] P. C. Dey, R. Das, Enhanced Photocatalytic Degradation of Methyl Orange Dye on Interaction with Synthesized Ligand Free CdS Nanocrystals under Visible Light Illumination, Spectrochimica Acta Part A: Molecular and Biomolecular Spectroscopy, Vol. 231, 2020, pp. 118122, https://doi.org/10.1016/j.saa.2020.118122.

[3] C. Namasivayam, D. Kavitha, Removal of Congo Red from Water by Adsorption onto Activated Carbon Prepared from Coir Pith, An Agricultural Solid Waste, Dyes and Pigments, Vol. 54, 2002, pp. 47-58, https://doi.org/10.1016/S0143-7208(02)00025-6.

[4] S. Shabbir, M. Faheem, N. Ali, P. G. Kerr, Y. Wu, Periphyton Biofilms: A Novel and Natural Biological System for the Effective Removal of Sulphonated Azo Dye Methyl Orange by Synergistic Mechanism, Chemosphere, Vol. 167, 2017, pp. 236-246, https://doi.org/10.1016/j.chemosphere.2016.10.002.

[5] L. Wang, L. Liu, Z. Zhang, B. Zhao, J. Li, B. Dong, N. Liu, 17α-Ethinylestradiol Removal from Water by Magnetic Ion Exchange Resin, Chinese Journal of Chemical Engineering, Vol. 26, 2018, pp. 864-869, https://doi.org/10.1016/j.cjche.2017.08.006.

[6] D. Tekin, Photocatalytic Degradation of Textile Dyestuffs Using TiO_2 Nanotubes Prepared by Sonoelectrochemical Method, Applied Surface Science, Vol. 318, 2014, pp. 132-136, https://doi.org/10.1016/j.apsusc.2014.02.018.

[7] N. Tripathy, R. Ahmad, J. E. Song, H. A. Ko, Y.-B. Hahn, G. Khang, Photocatalytic Degradation of Methyl Orange Dye by ZnO Nanoneedle under UV Irradiation, Materials Letters, Vol. 136, 2014, pp. 171-174, https://doi.org/10.1016/j.matlet.2014.08.064.

[8] V. A. Tran, A. N. Kadam, S. W. Lee, Adsorption-Assisted Photocatalytic Degradation of Methyl Orange Dye by Zeolite-Imidazole-Framework-Derived Nanoparticles, Journal of Alloys and Compounds, Vol. 835, 2020, pp. 155414, https://doi.org/10.1016/j.jallcom.2020.155414.

[9] S. Chen, J. Zhu, X. Wu, Q. Han, X. Wang, Graphene Oxide− MnO_2 Nanocomposites for Supercapacitors, ACS Nano, Vol. 4, 2010, pp. 2822-2830, https://doi.org/10.1021/nn901311t.

[10] D. V. Thanh, P. P. Oanh, P. H. Le, Ultrasonic-assisted Cathodic Electrochemical Discharge for Graphene Synthesis, Ultrasonics Sonochemistry, Vol. 34, 2017, pp. 978-983, https://doi.org/10.1016/j.ultsonch.2016.07.025.

[11] C. Julien, M. Massot, R. B. Hadjean, S. Franger, S. Bach, J. P. Ramos, Raman Spectra of Birnessite Manganese Dioxides, Solid State Ionics, Vol. 159, 2003, pp. 345-356, https://doi.org/10.1016/S0167-2738(03)00035-3.

[12] M. K. Rabchinskii, V. V. Shnitov, A. T. Dideikin, A. E. Aleksenskii, S. P. Vul', M. V. Baidakova, I. I. Pronin, D. A. Kirilenko, P. N. Brunkov, J. Weise, Nanoscale Perforation of Graphene Oxide During Photoreduction Process in The Argon Atmosphere, The Journal of Physical Chemistry C, Vol. 120, 2016, pp. 28261-28269, https://doi.org/10.1021/acs.jpcc.6b08758.

[13] C. Pan, H. Gu, L. Dong, Synthesis and Electrochemical Performance of Polyaniline@ MnO_2/Graphene Ternary Composites for Electrochemical Supercapacitors, Journal of Power Sources, Vol. 303, 2016, pp. 175-181, https://doi.org/10.1016/j.jpowsour.2015.11.002.

[14] H. Visser, C. E. Dubé, W. H. Armstrong, K. Sauer, V. K. Yachandra, FTIR Spectra and Normal-mode Analysis of A Tetranuclear Manganese Adamantane-Like Complex in Two Electrochemically Prepared Oxidation States: Relevance to The Oxygen-Evolving Complex of Photosystem II, Journal of The American Chemical Society, Vol. 124, 2002, pp. 11008-11017, https://doi.org/10.1021/ja020409j.

[15] H. A. Chu, H. Sackett, G. T. Babcock, Identification of a Mn-O-Mn Cluster Vibrational Mode of the Oxygen-Evolving Complex in Photosystem II by Low-Frequency FTIR Spectroscopy, Biochemistry, Vol. 39, 2000, pp. 14371-14376, https://doi.org/10.1021/bi001751g.